JACS
JOURNAL OF THE AMERICAN CHEMICAL SOCIETY

Communication

pubs.acs.org/JACS

A Reaction-Based Fluorescent Probe for Imaging of Formaldehyde in Living Cells

Aaron Roth,[†] Hao Li,[†] Chelsea Anorma, and Jefferson Chan*

Department of Chemistry, Roger Adams Laboratory, University of Illinois, 600 South Mathews, Urbana, Illinois 61801, United States

Web-Enhanced Feature Supporting Information

ABSTRACT: Formaldehyde (FA), in the 0.2−0.4 mM range, is produced and maintained endogenously via enzymatic pathways. At these levels, FA can promote cell proliferation as well as mediate memory formation. Once elevated, FA stress is known to induce cognitive impairments, memory loss, and neurodegeneration owing to its potent DNA and protein cross-linking mechanisms. Optical imaging is a powerful noninvasive approach used to study FA in living systems; however, biocompatible chemical probes for FA are currently lacking. Herein, we report the design, synthesis, and biological evaluation of Formaldehyde Probe 1 (FP1), a new fluorescent indicator based on the 2-aza-Cope sigmatropic rearrangement. The remarkable sensitivity, selectivity, and photostability of FP1 has enabled us to visualize FA in live HEK293TN and Neuroscreen-1 cells. We envision that FP1 will find widespread applications in the study of FA associated with normal and pathological processes.

Formaldehyde (FA) is a highly reactive carbonyl species recognized for its applications as a tissue fixative and embalming agent due to its potent capacity to cross-link DNA and protein through formation of stable methylene bridges. Exposure to exogenous FA via inhalation or ingestion poses a significant threat to human health. FA overload, for instance, can damage the central nervous system leading to reduced performance in memory and cognitive abilities.[1,2] However, the endogenous production of FA is a normal physiological process mediated by enzymatic systems such as semicarbazide-sensitive amine oxidase (SSAO) that generate FA and opposing molecular mechanisms that remove it.[3] In the brains of healthy individuals, the concentration of FA is in the 0.2−0.4 mM range[4] and has been proposed to play a role in the storage, preservation, and retrieval of long-term memory through DNA demethylation cycles.[5] However, FA is elevated in patients afflicted with neurodegenerative diseases such as Alzheimer's disease (AD) due to an overexpression of SSAO.[6] Indeed, abnormally high levels of FA, 0.5 mM, were found in the brain tissues of AD animal models.[7] In this context, FA is neurotoxic and has been shown to degrade neuronal networks through induction of hyperphosphorylation and polymerization of the τ protein.[8] Additionally, FA was reported to induce β-amyloid misfolding and aggregation via intramolecular and intermolecular cross-linking between lysine residues (Lys16 and Lys28).[9]

An assortment of methods including colormetric assays,[10] HPLC,[11,12] and GC[13] analyses following chemical derivatization, radiometric assays,[14] and mass spectrometry[15] analyses have been developed to measure levels of endogenous FA. However, these techniques either lack sensitivity or require the invasive destruction of biological tissue. Optical imaging is a powerful noninvasive alternative because it can be applied in living systems with minimal perturbation. Small-molecule probes that make use of biorthogonal chemical transformations have been employed to detect a variety of bioanalytes[16] ranging from gasotransmitters such as carbon monoxide[17,18] and hydrogen sulfide[19] to metal ions including iron[20] and zinc [21] as well as carbonyl metabolites like methylglyoxal.[22] However, no such imaging agents were previously available for in cellulo imaging of FA.[23] We now present a new approach for the detection of FA in live cells through the development of Formaldehyde Probe 1 (FP1), a FA-responsive fluorescent indicator which is comprised of three discrete elements: a fluorescent core (Figure 1, in black), a FA reactive moiety (Figure 1, in blue), and a dark quencher (Figure 1, in red).[24]

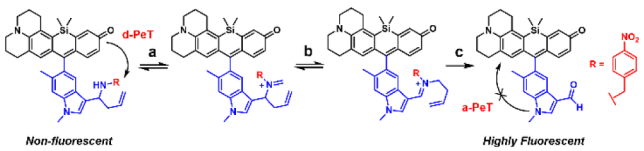

Figure 1. A new formaldehyde detection strategy based on the 2-aza-Cope sigmatropic rearrangement. The R group in red designates the 4-nitrobenzyl dark quencher moiety. Labels a, b, and c represent condensation with formaldehyde, rearrangement, and hydrolysis steps, respectively.

A new julolidine-based silicon rhodol fluorescent scaffold was developed for the construction of FP1. This fluorophore exhibits an absorption maximum centered at 633 nm, which lies precisely on the 633 nm HeNe laser line commonly found in many confocal microscopes and flow cytometers. Such red-shifted fluorophores are desirable because of low autofluorescence, minimal phototoxicity, and negligible interference from biomolecules when employed in live cell imaging. In order to optimize the detection sensitivity, our design involves minimizing the background fluorescence of FP1 by appending a 4-nitrobenzyl group known to abolish fluorescence through a donor-excited PeT (d-PeT) process.[25] Indeed, installation of this dark quencher moiety reduces the quantum efficiency (Φ_F) from 0.02 for precursor **5** to undetectable levels for FP1 (Table S1). In

Received: May 22, 2015
Published: August 25, 2015

DOI: 10.1021/jacs.5b05339
J. Am. Chem. Soc. 2015, 137, 10890−10893

the presence of FA, a reversible condensation event yields an iminium intermediate which can undergo a charge-promoted [3,3]-sigmatropic rearrangement−hydrolysis sequence to expel the aryl nitro group and afford a highly fluorescent indole-3-carboxaldehyde product (Φ_F = 0.11) (Table S1). Of note, the aldehyde is strategically positioned at C3 such that after the reaction cascade, the N1 lone pair electrons can delocalize into the π-system rather than quench fluorescence via an acceptor-excited PeT (a-PeT) pathway. In this regard, silicon rhodol **3**, without the carboxaldehyde, is nonfluorescent (Table S1).

To this end, FP1 was synthesized beginning with the reaction between indole **2** and *tert*-butyllithium to afford a lithium adduct which could subsequently react with silicon xanthone **1**. Silicon rhodol **3** was obtained after sequential acid-mediated dehydration and BBr_3 demethylation reactions. The indole moiety was subjected to Vilsmeier−Haack formylation conditions to furnish carboxaldehyde **4** which was transformed to the homoallylic amine **5** with potassium allyltrifluoroborate in methanolic ammonia. Lastly, reductive amination with 4-nitrobenzaldehyde and triacetoxyborohydride yields FP1 (Scheme 1).

Scheme 1. Synthesis of FP1

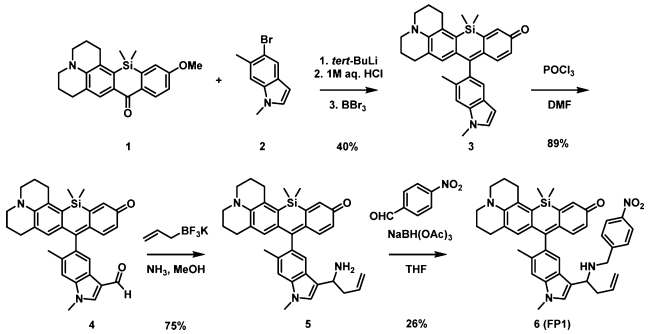

We then evaluated the fluorescence properties of FP1 in PBS buffer (pH 7.4) in response to FA. Prior to FA treatment, a 1 μM solution of FP1 is almost nonfluorescent; however, upon addition of FA, a dose-dependent fluorescence increase was observed (Figure S1). For example, upon treatment with 0.25 mM FA, within reported physiological levels in the brain, a ~7.0-fold fluorescence increase was observed after 3 h at 37 °C (Figure 2a), whereas 5 mM FA triggered a larger ~33.5-fold enhancement (Figure S1). Additionally, the lower limit of detection of FP1 after 3 h incubation at 37 °C was determined to be 0.01 mM FA using standard protocols.[26] Given the highly reactive nature of the aldehyde functionality, we examined whether biologically relevant aldehyde containing species such as acetaldehyde, glucose, methylglyoxal, and pyridoxal would cross-react with FP1 to give false positive results. When 1 μM FP1 was reacted with 1 mM of the various analytes, we observed only minimal cross-reactivity. In the case of acetaldehyde, a 1.9-fold fluorescence increase was detected after 3 h (Figure 2b). In contrast, treatment with FA at the same concentration resulted in a 12.8-fold signal enhancement. Moreover, because FP1 contains an aryl nitro group which may be reduced by thiols such as cysteine, glutathione, and hydrogen sulfide[27] to the corresponding aniline product, we examined the chemical stability of FP1 in the presence of these intracellular reductants and observed no aberrant reactivity (Figure 2b). In addition to its ability to cross-link biomolecules, FA is cytotoxic through the induction of oxidative stress.[28] Thus, we reacted FP1 with 1 mM hydrogen peroxide, a common reactive oxygen species, to mimic oxidative stress in cells but found no significant change in fluorescence (Figure 2b). The emission spectra of FP1 were recorded at a variety of pH values ranging from 2.0 to 10.4; however, owing to its weak emission, a reliable pH-fluorescence trace could not be obtained. As such, we constructed the corresponding pH profile for carboxaldehyde **4** and noted that the high fluorescence intensity was maintained under physiological conditions (Figure S2).

After demonstrating excellent responsiveness to FA and exceptional selectivity in vitro, we tested the ability of FP1 to visualize FA in live cells. Prior to examining physiological concentrations, it was essential for us to first validate our assay parameters using FA levels that would yield high contrast while maintaining cell viability. To this end, HEK293TN cells were incubated with 2 μM FP1 at 37 °C for 8 min and then treated with buffer alone or buffer containing FA at 1, 2.5, or 5 mM for 3 h. Prior to imaging, cells were allowed to recover in FA-free buffer for 30 min. As shown in Figure 3a−d and quantified in Figure 3e, treatment of HEK293TN cells with FA resulted in a dose-dependent increase in fluorescence. At 5 mM FA, a nearly 3-fold fluorescence increase was recorded. Likewise, a time-dependent turn-on response at each FA concentration was observed (Figures S3 and S4). Having established the utility of FP1 in live HEK293TN cells, we turned our attention to Neuroscreen-1

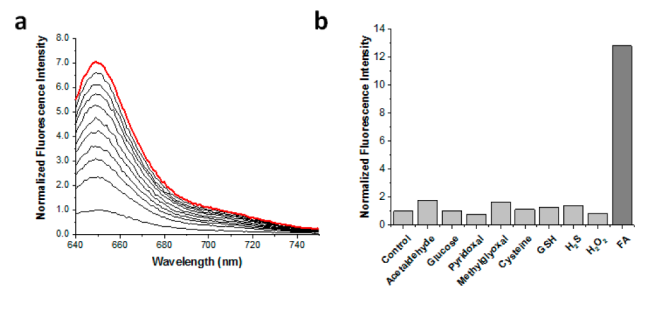

Figure 2. (a) Fluorescence response of 1 μM FP1 to 0.25 mM FA in PBS buffer (pH 7.4) at 37 °C. FP1 was excited at 633 nm, and the emission was collected between 640 and 750 nm. Time points are 0, 15, 30, 45, 60, 75, 90, 105, 120, 150, and 180 min. (b) Fluorescence response of 1 μM FP1 to biologically relevant aldehydes, reactive sulfur species, and hydrogen peroxide. Bars represent normalized fold changes in response to treatment with each analyte listed at 1 mM for 3 h.

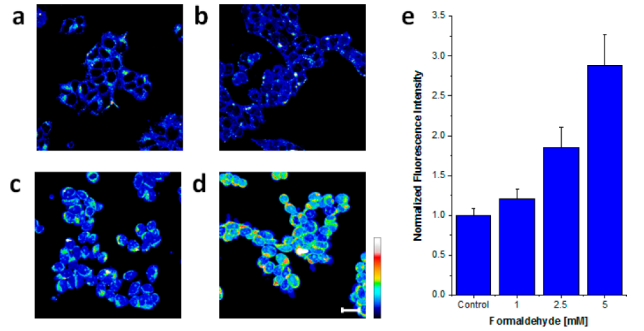

Figure 3. Confocal microscopy images acquired by irradiation of HEK293TN cells treated with (a) a DMEM vehicle control, (b) 1, (c) 2.5, and (d) 5 mM FA for 3 h at 37 °C with the 633 nm HeNe laser. Scale bar represents 20 μm. Pseudocoloring represents intensity distribution from highest intensity indicated by white to the lowest intensity designated by black. (e) Quantification of imaging data.

DOI: 10.1021/jacs.5b05339
J. Am. Chem. Soc. 2015, 137, 10890−10893

(NS1) cells, a subclone of the PC12 cell-line which is recognized as a standard neuronal model system.[29] As was the case with HEK293TN cells, incubation of NS1 cells with 1, 2.5, or 5 mM FA at 37 °C for 3 h gave rise to a robust dose-dependent signal enhancement of up to 2.3-fold (Figure 4a–d) as well as a time-dependent turn-on response at each concentration (Figures S5 and S6). We confirmed via HR-MS that the fluorescence increase resulted from conversion of FP1 to carboxyaldehyde **4** by reacting FP1 with 5 mM FA in the presence of cellular lysates (Figure S14). Because FA is a powerful fixative, we performed cell viability assays to determine the cytotoxicity of FA under our experimental conditions. We employed a dye exclusion protocol utilizing trypan blue to selectively stain and distinguish dead cells from those that were viable. At 1 mM FA, only 5% of the HEK293TN cells were dead after 3 h, whereas nearly 35% of cells were no longer viable at 5 mM FA (Figure S8a). NS1 cells on the other hand were remarkably resilient when incubated with FA up to 2.5 mM. Specifically, at this concentration there was only ~12% loss in viability after 3 h. However, incubation with 5 mM FA resulted in considerable cell death (Figure S8b). To further verify that the cell populations under investigation were indeed alive, DAPI, a cell permeable nuclear and chromosome counterstain, was employed to identify intact nuclei (Figure S9).

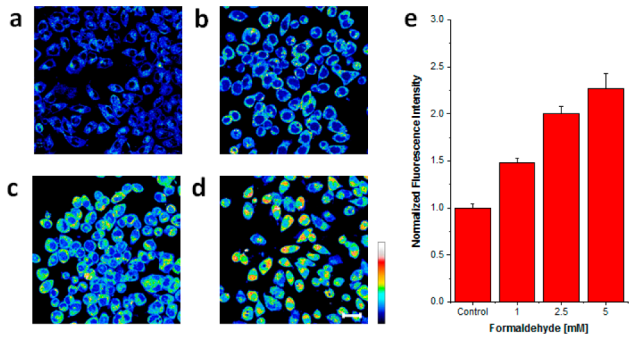

Figure 4. Confocal microscopy images acquired by irradiation of NS1 cells treated with (a) a vehicle control, (b) 1, (c) 2.5, and (d) 5 mM FA at 37 °C for 3 h with the 633 nm HeNe laser. Scale bar represents 20 μm. Pseudocoloring represents intensity distribution from highest intensity indicated by white to the lowest intensity designated by black. (e) Quantification of imaging data.

It was essential to determine the staining pattern of FP1 because enzymes that produce endogenous FA exhibit unique subcellular localization patterns. For example, SSAO is primarily localized to the plasma membrane.[30] Thus, we costained both HEK293TN and NS1 cells with ER-Tracker Green, LysoTracker Green DND-26, and MitoTracker Green FM, fluorescent indicators that are known to selectively stain the endoplasmic reticulum, lysosome, and mitochondria, respectively, in almost all cell types (Figures S10 and S11). From these imaging experiments, it was evident that FP1 stained the cytoplasm as well as the endoplasmic reticulum in both cell lines as judged by excellent fluorescence overlay with ER-Tracker Green. In contrast, FP1 did not co-localize with the lysosomal or mitochondrial stains. Additionally, we performed an assay to determine dye efflux properties. HEK293TN and NS1 cells were stained with 1 μM FP1 for 8 min and then washed with fresh dye-free buffer. Images were acquired after a 30 min recovery period and then again after 8 h. We found that there was no statistically significant decrease in fluorescence, suggesting that FP1 is chemically stable and does not efflux into the cell media (data not shown). We then examined the photostability of FP1 toward repeated irradiation cycles. To our delight, there was no decrease in fluorescence after 100 scans at 25% laser power with a pinhole size of 1 airy unit (Figure S12). Of note, 3% laser power is routinely used for all other imaging experiments described in this study. Owing to the exquisite photostability of FP1, we were motivated to perform a time-lapse imaging experiment in live NS1 cells. For this experiment, NS1 cells were stained with 1 μM FP1 as previously described followed by on-stage addition of 1 mM FA at 25 °C. Images were then acquired every min for 2 h (Movie 1). Under these conditions we observed a 1.3-fold fluorescence increase; however, we also noted a FA-induced cell rounding effect which could be reversed during a 30 min recovery period.

To corroborate our confocal imaging data, we turned to flow cytometry because this high-throughput technique allows for the rapid quantification of large cell populations. As such, HEK293TN and NS1 cells were stained with FP1 as previously described and then incubated with 1, 2.5, and 5 mM FA for up to 3 h. As with confocal imaging, we observed a concentration- and time-dependent fluorescence signal enhancement (Figures S13 and S14). Indeed, there was a clear and unambiguous shift in the live cell population when FA was applied. Based on the median APC-A fluorescence intensity values (an APC-A filter set was used), treatment of HEK293TN cells with 5 mM FA at 37 °C for 3 h resulted in nearly a 2.5-fold turn-on, which is in excellent agreement with the confocal imaging assays of 2.9-fold (Figure 5a). In contrast, NS1 cells incubated with 5 mM FA afforded a 4.2-fold increase by flow cytometry, whereas only a 2.3-fold turn-on was noted using confocal microscopy (Figure 5b). This discrepancy can be attributed to the cytotoxicity of FA at this concentration which reduces the fluorescence of dead cells due to dye leakage. Thus, a lower apparent turn-on was recorded because it is difficult to image only viable cells in the presence of those that are dead.

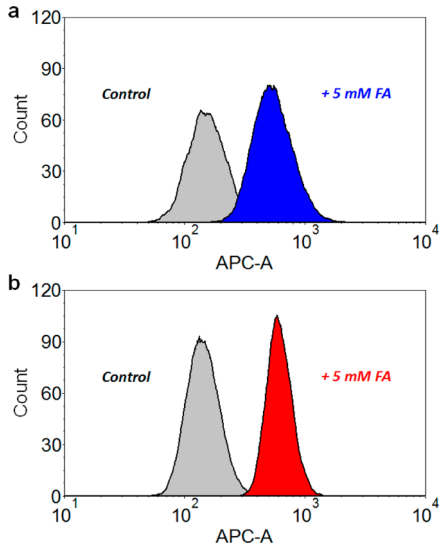

Figure 5. Flow cytometry analysis of (a) HEK293TN and (b) NS1 cells stained with 1 μM FP1 and incubated with 5 mM FA at 37 °C for 3 h. Excitation was provided by the 633 nm HeNe laser, and an APC-A filter set was applied. Only live cells were counted.

To demonstrate that FP1 possessed sufficient sensitivity to detect physiologically relevant levels of FA, we repeated our confocal imaging and flow cytometry assays by treating living

DOI: 10.1021/jacs.5b05339
J. Am. Chem. Soc. 2015, 137, 10890–10893

NS1 cells stained with FP1 with 0.25 and 0.5 mM FA. As with higher concentrations of FA, incubation of NS1 cells with 0.25 and 0.5 mM FA at 37 °C for 3 h afforded a dose-dependent signal enhancement of 16% and 38%, respectively (Figure S15). Likewise, flow cytometry analyses of NS1 cells incubated with 0.25 and 0.5 mM resulted in a 42% and 50% fluorescence turn-on, respectively (Figure S16). Moreover, we anticipate extended incubation beyond the 3 h time point will result in improved contrast because a larger fraction of FP1 will have sufficient time to react with FA. These crucial experiments validate the utility of FP1 for detection of FA at endogenous levels and, thus, provides us with unique opportunities to study both normal and pathological systems.

In summary, we have developed a new fluorescent probe, FP1, for imaging FA using the 2-aza-Cope sigmatropic rearrangement. We strategically incorporated a 4-nitrobenzyl dark quencher to reduce background fluorescence via d-PeT. The ensuing product features an aldehyde moiety at the C3 indole position which enhances fluorescence and, thus, the dynamic range through perturbation of a-PeT quenching. As such, the high sensitivity of FP1 enabled us to detect FA in vitro at concentrations below those reported in the brain. In addition, FP1 was successfully used to image physiological levels of FA in live HEK293TN and NS1 cells in a dose- and time-dependent manner. Of note, we developed a new julolidine-based silicon rhodol fluorescent scaffold which features an absorption maxima centered at 633 nm. This property enabled us to excite FP1 with the 633 nm HeNe laser in both confocal microscopy and flow cytometry experiments. Moreover, because FP1 exhibits excellent photostability, we performed a time-lapse imaging experiment where the reaction between FP1 and FA could be captured in real-time. Taken together, this study demonstrates that FP1 will find utility in elucidating the physiological roles of FA in live cells.

■ ASSOCIATED CONTENT

Supporting Information

The Supporting Information is available free of charge on the ACS Publications website at DOI: 10.1021/jacs.5b05339.

Experimental details, including synthesis of **1**−**5** and **FP1** and all data for in vitro and in cellulo experiments are presented (PDF)

Web-Enhanced Feature

A time-lapse imaging movie of the reaction between FP1 and FA in AVI format is available in the online version of the paper.

■ AUTHOR INFORMATION

Corresponding Author

*jeffchan@illinois.edu

Author Contributions

†These authors contributed equally.

Notes

The authors declare no competing financial interest.

■ ACKNOWLEDGMENTS

We thank Profs. Paul Hergenrother (UIUC Department of Chemistry) and Kai Zhang (UIUC Department of Biochemistry) for generously supplying HEK293TN and NS1 cells, respectively. Furthermore, we thank Dr. Sandy McMasters (UIUC Cell Media Facility) for her technical expertise. A.R. and C.A. acknowledge the National Institute of General Medical Sciences (NIGMS)-NIH Chemistry-Biology Interface Training Grant (5T32-GM070421). C.A. thanks the Robert C. and Carolyn J. Springborn Endowment and the UIUC Graduate College for graduate fellowships.

■ REFERENCES

(1) Songur, A.; Ozen, O. A.; Sarsilmaz, M. *Rev. Environ. Contam T* **2010**, *203*, 105.
(2) Tulpule, K.; Dringen, R. *J. Neurochem.* **2013**, *127*, 7.
(3) O'Sullivan, J.; Unzeta, M.; Healy, J.; O'Sullivan, M. I.; Davey, G.; Tipton, K. F. *NeuroToxicology* **2004**, *25*, 303.
(4) Tong, Z. Q.; Han, C. S.; Luo, W. H.; Wang, X. H.; Li, H.; Luo, H. J.; Zhou, J. N.; Qi, J. S.; He, R. Q. *Age* **2013**, *35*, 583.
(5) Tong, Z. Q.; Han, C. S.; Luo, W. H.; Li, H.; Luo, H. J.; Qiang, M.; Su, T.; Wu, B. B.; Liu, Y.; Yang, X.; Wan, Y.; Cui, D. H.; He, R. Q. *Sci. Rep.* **2013**, *3*.
(6) Unzeta, M.; Sole, M.; Boada, M.; Hernandez, M. *J. Neural Transm* **2007**, *114*, 857.
(7) Tong, Z. Q.; Zhang, J. L.; Luo, W. H.; Wang, W. S.; Li, F. X.; Li, H.; Luo, H. J.; Lu, J.; Zhou, J. N.; Wan, Y.; He, R. Q. *Neurobiol. Aging* **2011**, *32*, 31.
(8) Lu, J.; Miao, J. Y.; Su, T.; Liu, Y.; He, R. Q. *Biochim. Biophys. Acta, Gen. Subj.* **2013**, *1830*, 4102.
(9) Chen, K.; Maley, J.; Yu, P. H. *J. Neurochem.* **2006**, *99*, 1413.
(10) Nash, T. *Biochem. J.* **1953**, *55*, 416.
(11) Soman, A.; Qiu, Y.; Li, Q. C. *J. Chromatogr. Sci.* **2008**, *46*, 461.
(12) Su, T.; Wei, Y.; He, R. Q. *Shengwu Huaxue Yu Shengwu Wuli Jinzhan* **2011**, *38*, 1171.
(13) Janos, E.; Balla, J.; Tyihak, E.; Gaborjanyi, R. *J. Chromatogr.* **1980**, *191*, 239.
(14) Szarvas, T.; Szatloczky, E.; Volford, J.; Trezl, L.; Tyihak, E.; Rusznak, I. *J. Radioanal. Nucl. Chem.* **1986**, *106*, 357.
(15) Kato, S.; Burke, P. J.; Koch, T. H.; Bierbaum, V. M. *Anal. Chem.* **2001**, *73*, 2992.
(16) Chan, J.; Dodani, S. C.; Chang, C. J. *Nat. Chem.* **2012**, *4*, 973.
(17) Wang, J.; Karpus, J.; Zhao, B. S.; Luo, Z.; Chen, P. R.; He, C. *Angew. Chem., Int. Ed.* **2012**, *51*, 9652.
(18) Michel, B. W.; Lippert, A. R.; Chang, C. J. *J. Am. Chem. Soc.* **2012**, *134*, 15668.
(19) Lin, V. S.; Lippert, A. R.; Chang, C. J. *Proc. Natl. Acad. Sci. U. S. A.* **2013**, *110*, 7131.
(20) Hirayama, T.; Okuda, K.; Nagasawa, H. *Chem. Sci.* **2013**, *4*, 1250.
(21) Chyan, W.; Zhang, D. Y.; Lippard, S. J.; Radford, R. J. *Proc. Natl. Acad. Sci. U. S. A.* **2014**, *111*, 143.
(22) Wang, T. N.; Douglass, E. F.; Fitzgerald, K. J.; Spiegel, D. A. *J. Am. Chem. Soc.* **2013**, *135*, 12429.
(23) Song, H.; Rajendiran, S.; Kim, N.; Jeong, S. K.; Koo, E.; Park, G.; Thangadurai, T. D.; Yoon, S. *Tetrahedron Lett.* **2012**, *53*, 4913.
(24) Brewer, T. F.; Chang, C. J. *J. Am. Chem. Soc.* **2015**, DOI: 10.1021/jacs.5b05340.
(25) Ueno, T.; Urano, Y.; Kojima, H.; Nagano, T. *J. Am. Chem. Soc.* **2006**, *128*, 10640.
(26) Little, T. A. *Biopharm Int.* **2015**, *28*, 48.
(27) Montoya, L. A.; Pluth, M. D. *Chem. Commun.* **2012**, *48*, 4767.
(28) Zararsiz, I.; Kus, I.; Ogeturk, M.; Akpolat, N.; Kose, E.; Meydan, S.; Sarsilmaz, M. *Cell Biochem. Funct.* **2007**, *25*, 413.
(29) Greene, L. A.; Tischler, A. S. *Proc. Natl. Acad. Sci. U. S. A.* **1976**, *73*, 2424.
(30) Andres, N.; Lizcano, J. M.; Rodriguez, M. J.; Romera, M.; Unzeta, M.; Mahy, N. *J. Histochem. Cytochem.* **2001**, *49*, 209.

DOI: 10.1021/jacs.5b05339
J. Am. Chem. Soc. 2015, 137, 10890−10893